Axial Diffusion and Pressure Drop of Liquids in Porous Media

E. P. STAHEL and C. J. GEANKOPLIS

The Ohio State University, Columbus, Ohio

Much experimental data exist on axial or longitudinal diffusion or dispersion coefficients of liquids in unconsolidated media of packed beds of spheres or tower packing. Recently Ebach and White (*11*), Carberry and Bretton (*7*), Strang and Geankoplis (*23*), and Liles and Geankoplis (*13*) obtained D_L data on packed beds of spheres in sizes from 0.21 to 6.1 mm. It was concluded (*13*) that because of the large spread of experimental data there was general agreement between all investigators. The effect of diameter of particle d_p remains inconclusive since contradictory effects were found (*7, 11, 13*).

It was shown (*13*) that if void analytical sections are not used, there is no effect of bed length L on D_L. For lengths above about 60 cm. little end effects were found when void analytical sections were used.

Cairns and Prausnitz (*5, 6*) studied the effect of a nonflat velocity profile on D_L in a packed bed of spheres and showed that the average D_L is slightly greater than the point D_L. This relationship was also derived by Converse (*9*). If the ratio of bed diameter to d_p is 15/1 or greater, the velocity profile is essentially flat.

Turner (*29, 30*) has derived equations for D_L for two physical models. In model 1 he uses a main flow channel with side dead-end pockets, and in model 2 he uses three parallel channels of different lengths which are mixed at the end in a header. His experimental results are the only ones in the literature for which the exact physical geometries are known and for which theoretical equations have been derived. Aris (*1, 2*) later modified Turner's equations slightly.

Only few experimental data exist for D_L of liquids in unconsolidated irregular structures such as sand beds. Beran (*3*), Rafai (*16*), and Von Rosenberg (*31*) present data for sand beds with liquids with the results in some cases differing widely. Blackwell (*4*) summarizes these data and shows that at values of $d_p\,U/D$ less than 0.08 the D_L is constant and is approximately equal to $D/1.5$, where 1.5 is a tortuosity factor. At values above 0.08 the D_L is proportional to $U^{1.17}$, and molecular diffusion is of little importance.

In the majority of cases pressure drop in these beds of spheres or sand were not measured, so comparisons of momentum transfer and axial diffusion were not made. However Carberry and Bretton (*7*) did measure pressure drop and D_L in packed beds of spheres and state that at a value of N'_{Re} of about 400 the D_L value does not rise as fast as at lower Reynolds numbers. This point corresponds approximately to the point of transition from laminar to turbulent flow in their friction factor f vs. N'_{Re} plot. Tek (*28*) gives a plot of friction factor vs. Reynolds number for various unconsolidated sands.

E. P. Stahel is at North Carolina State University, Raleigh, North Carolina.

In the present work D_L values were obtained for water flowing through random consolidated porous media using frequency response techniques. The porous media were made by pouring Wood's metal over a packed bed of salt crystals and leaching out the salt. This yielded in effect a porous solid which was essentially the inside out or reverse of a packed bed with the size of the large void chambers known.

Pressure drop data were obtained and correlated by the Ergun (*12*) equation and related to D_L.

THEORY

Axial Diffusion

The basic theory for the frequency response method has been derived by Rosen and Winsche (*17*) and modified by others (*7, 10, 11, 13, 14*). When one follows their derivations, the basic differential equation is

$$D_L \frac{\partial^2 C}{\partial Z^2} - \frac{U \partial C}{\partial Z} = \frac{\partial C}{\partial t} \tag{1}$$

Using a continuous sine wave input to the bed, putting in the appropriate boundary conditions, and integrating one obtains

$$B = -\frac{UL}{2D_L}\left\{1 - \sqrt{\sqrt{\frac{1}{4} + \left(\frac{2\,D_L\,\omega}{U^2}\right)^2} + \frac{1}{2}}\right\} \tag{2}$$

When one expands Equation (2) in a series and drops higher-order terms, the simplified form results:

$$B = \frac{L\,\omega^2\,D_L}{U^3} \tag{3}$$

The equation for the phase shift referred to the entrance of the bed is

$$\zeta_{\text{Calc}} = \frac{UL}{2D_L}\sqrt{\sqrt{\frac{1}{4} + \left(\frac{2\,D_L\,\omega}{U^2}\right)^2} - \frac{1}{2}} \tag{4}$$

Expanding Equation (4) and dropping higher-order terms one gets

$$\zeta_{\text{Calc}} = \frac{\omega L}{U} \tag{5}$$

To predict the D_L in a circular flow channel with dead-end side pockets which is similar to Turner's model 1 Aris (*1, 2*) derived the following equation:

$$D_L = D + \frac{KUc^2\,a^2}{D} + \frac{Uc^2}{3D\,(1+\beta)^2}\int_o^\infty \beta(1)\,1^2\,dl \tag{6}$$

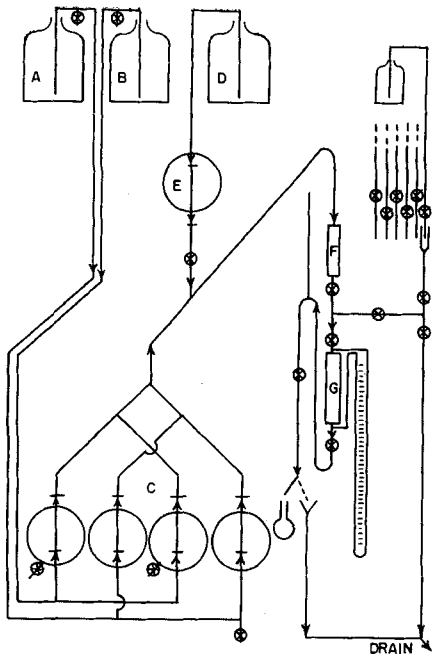

Fig. 1. Process flow diagram.

where

$$K = \frac{1 + 6\beta + 11\beta^2}{48\ (1 + \beta)^2} \tag{7}$$

If β is zero, that is no dead-end side pockets, Equation (6) reduces to Taylor's Equation (8) (25, 26) for D_L in laminar flow in a tube:

$$D_L = D + \frac{Uc^2\, a^2}{48\, D} \tag{8}$$

For a random porous medium at low velocities in the laminar region attempts have been made to predict D_L for equivalent capillaries in various arrangements with Taylor's equation. Saffman (18, 19) has derived a theory using a network of capillaries and gets an approximate solution which he states checks experimental data approximately but does not include any dead-end pockets in his analysis. Scheidegger (20) reviews and discusses other such models. However the main drawback to checking these theories is that the exact porous structure geometry of the random media is not known.

Pressure Drop

Scheidegger (20) and Streeter (24) review the equations for pressure drop in porous media. The generally accepted equation for flow in porous media in laminar flow or Reynolds numbers less than about 1.0 is the Darcy equation, where k is the specific permeability in square centimeters.

$$\frac{\Delta P}{L} = \frac{\mu}{k} q \tag{9}$$

For higher velocities Ergun (12) and Tek (28) have derived the following for a given liquid and porous solid.

$$\frac{\Delta P}{L} = \frac{\mu}{k} q + K_2 q^2 \tag{10}$$

The second term on the right side of the equation represents the kinetic energy losses and the first term the viscous energy losses.

The friction factor is defined by others (12, 15, 28) as

$$f = \frac{\Delta P\, d_p\, g_c}{L\, 2\, \rho\, (U')^2} \tag{11}$$

The pressure drop for laminar flow in a channel is given as

$$\Delta P' = \frac{32\, L\, Uc^2\, \rho}{N_{Rec}\, g_c\, dc\ 13.6} \tag{12}$$

There are several methods available in the literature to estimate the specific surface area S of a porous solid from the Darcy specific permeability (20). The simplest of these by Kozeny (20) is derived from the assumption of equivalent capillaries:

$$k = \frac{a'\, \epsilon^3}{S^2} \tag{13}$$

The Carman-Kozeny (20) equation is

$$k = \frac{\epsilon^3}{5\, S_o^2\, (1 - \epsilon)^2} \tag{14}$$

The modified Kozeny equation with a tortuosity factor T of 1.5 is

$$k = \frac{a'\, \epsilon^3}{T\, S^2} \tag{15}$$

EXPERIMENTAL METHODS

Apparatus

The apparatus shown in Figure 1 is a modification of that used by Liles and Geankoplis (13). The items are (A) and (D) water storage; (B) 2-naphthol or trace solution storage; (E) gear pump to increase the water flow and enable frequency to be varied independently of velocity; (C) four single-action positive-displacement pumps; (F) precalming section to remove higher harmonics in the inlet sine wave; and (G) test cell containing a calming section of glass beads, the porous solid, and a calming section at the outlet. The flow was measured by weighing timed amounts of the outlet water solution. A variable-drive cam-operated mechanism actuates the four pumps, and one revolution yields two sine wave periods.

Porous Media

The cylindrical shaped random porous media were made by first crushing and screening sodium chloride crystals to an average size of 1,000 μ and having a size range 18% smaller and 18% larger. Also, an average size of 2,000 μ was prepared having a size range of $\pm$ 18% This salt was added to a hollow metal cylinder mold and covered with a metal screen to keep it compact. Then Wood's metal was poured over the salt with a slight vacuum on the bottom of this mold. The metal completely filled the voids. After cooling the plug was machined in the form of a cylinder 1.00 in. in diameter and a length of 3.3 in. for the 1,000-μ plug and 4.4 in. for the 2,000-μ plug. Analytical slits 1/8 by 3/16 in. were drilled. No air bubbles were observed in the machined plug. The salt was then completely leached out with water.

The void fraction of the random porous solids was determined by weighing the solid before and after leaching, the weight difference being the salt removed. The reproducibility of each individual plug was such that a maximum deviation of 1.5% in void fraction was obtained for a set of plugs. The void fraction of the 1,000-μ plugs was 0.517 and 0.525 for the 2,000-μ plugs.

For the 2,000-μ sample three lengths were placed end to end as in (A) of Figure 2 in the cell holder. The two analytical holes are shown as (B) and (B') in Figure 2 and are 12.0 in. apart. The middle length of plug contained no analytical hole. The conical calming sections (G) and (F) were filled with glass beads 0.4 cm. in diameter, and the total length of both sections was 8.26 cm. Each hole (H) contained a window in the brass holders (E) and (E') for the analytical slit. A thin rubber sleeve (D) was used as a gasket fitting around the porous cylinder to make it water tight when the sides (E) and (E') were clamped together. For the 1,000-μ sample four lengths of porous plugs were used.

Similar small analytical slits were used successfully by Liles and Geankoplis (13) to eliminate end effects. The pressure

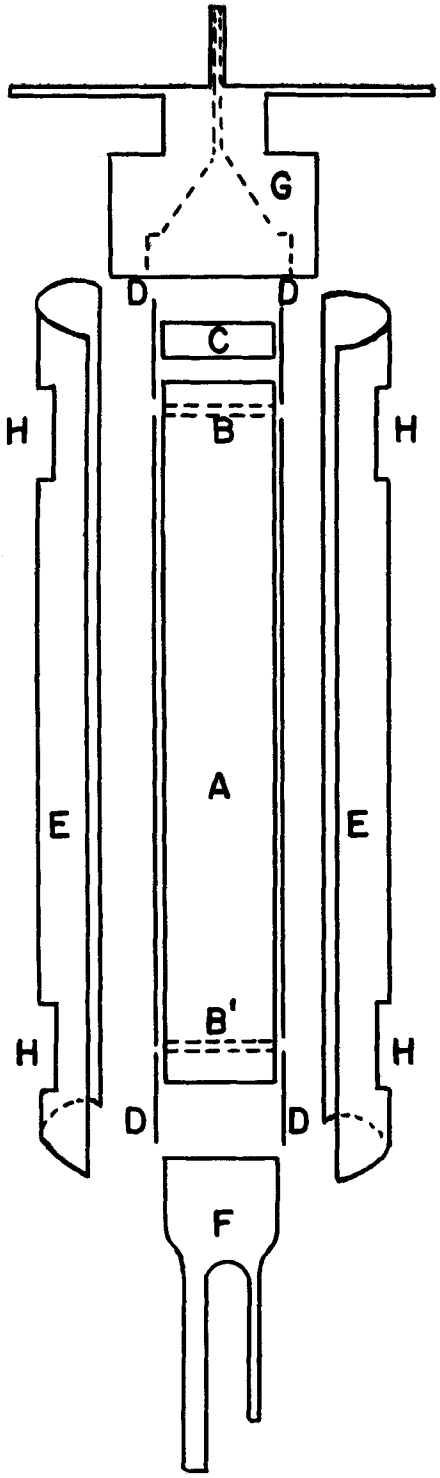

Fig. 2. Exploded schematic of cell holder and porous plug.

drop across the entire porous plug of 13.125 in. length plus the two calming sections at each end was measured by a manometer.

Analytical

The concentration of the tracer 2-naphthol in the solution passing through the porous plug (Figure 2) affects the amount of light passing through the slits and going to the photo tubes. Details are given elsewhere (22). The outputs of the photo tubes were recorded. The recorder was calibrated twice a day at the beginning and at the end of a series of runs by passing known solutions through with the maximum concentration of 2-naphthol of 20 parts/million. The inlet and outlet sine waves were very close to true sine waves (22).

Table 1. Experimental Data for Random Porous Media

Run no.	U	ω	D_L	N'_{Re}	$\frac{\Delta P'}{L}$	ζ_{Exp}	ζ_{Calc}
			1000 Micron Porous Solid				
87	1.556	0.3266	1.78	8.50	0.241	6.01	6.01
88	2.692	0.3266	4.43	14.70	0.518	3.57	3.46
89	3.53	0.3266	5.91	19.25	0.735	2.83	2.71
90	1.046	0.3266	0.960	5.71	0.111	9.14	9.15
91	2.147	0.3266	3.01	11.72	0.323	4.39	4.31
92	0.529	0.1505	0.581	2.89	0.0414	7.34	7.60
93	1.598	0.1505	—	8.72	0.215	—	—
94	3.08	0.2503	—	16.83	0.583	—	—
95	4.79	0.3644	—	26.13	1.060	—	—
96	3.28	0.3644	—	17.92	0.550	—	—
97	0.443	0.1089	0.436	2.419	0.0249	—	6.85
98	3.42	0.3307	5.84	18.67	0.630	3.34	2.81
99	5.03	0.3307	9.10	27.45	1.110	2.09	1.95
100	2.29	0.3307	3.85	12.50	0.323	4.07	4.02
101	4.17	0.3307	7.40	22.77	0.838	2.44	2.33
			2000 Micron Porous Solid				
72	2.59	0.2719	2.79	28.6	0.525	3.22	3.12
73	3.45	0.2719	4.73	38.2	0.830	2.44	2.35
74	1.840	0.2719	1.691	20.38	0.249	4.39	4.36
75	2.86	0.2719	3.33	31.7	0.627	2.92	2.83
76	4.13	0.2719	6.00	45.7	1.145	2.06	1.97
77	2.18	0.2747	2.12	24.3	0.415	4.06	3.74
78	1.130	0.2747	0.892	12.52	0.1295	6.98	6.97
79	0.872	0.2747	0.533	9.66	0.0773	9.00	9.03
80	4.04	0.3595	5.50	44.8	1.306	2.77	2.67
81	4.76	0.3595	6.51	52.8	1.555	2.35	2.28
82	1.500	0.3694	1.001	16.62	0.185	7.30	7.52
83	1.490	0.2501	1.12	16.52	0.182	4.95	4.94
84	1.490	0.1776	1.446	16.52	0.182	3.58	3.54
85	1.540	0.1275	1.490	17.08	0.182	2.50	2.49
86	1.500	0.0929	1.630	16.62	0.182	1.89	1.84

EXPERIMENTAL DATA AND CALCULATIONS

Experimental data are given in Table 1 for fifteen runs with the 1,000-μ porous medium and fifteen runs with the 2,000-μ porous medium. Detailed data are given elsewhere (22). The average temperature was 22.4°C. Velocity, frequency, and type of porous medium were varied.

The distance between two timing pips represents two periods on the plot containing the inlet and outlet sine waves. The phase shift was determined by measuring the distance between the 50% concentration points of the inlet and outlet waves. This enabled ξ_{exp} to be obtained. The ξ_{calc} was calculated from Equation (4). To calculate D_L Equation (2) was used since the simplified Equation (3) gave results in error.

The experimental pressure drop measurement for each run was corrected for the pressure drop of the glass beads in the calming sections before and after the random porous medium by using the plot in Perry's (15). This correction in all cases was less than 1%. The friction factor f was calculated from Equation (11). The specific surface areas of the random

Table 2. Specific Surface Areas of Random Porous Media

Porous medium	Specific permeability, k	S', specific surface area in sq. cm./g. Assuming A cube	Equation (13)	Equation (14)	Equation (15)	Sherwood, Pigford
1,000 μ	2.88×10^{-6}	8.0	33.0	20.9	27.0	6.13
2,000 μ	2.88×10^{-6}	4.3	34.9	21.7	28.5	3.08

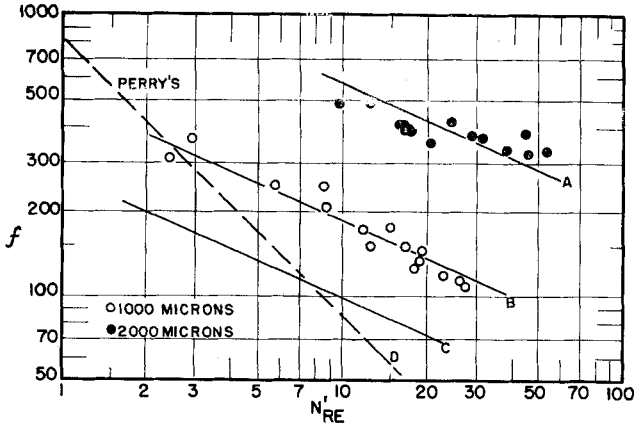

Fig. 3. Friction factor as a function of N_{RE}.

porous media were calculated from Equations (13), (14), and (15) and the method in Sherwood and Pigford (*21*) and are given in Table 2.

DISCUSSION

Frequency and Phase Angle

To find the effect of frequency on D_L for the 2,000-μ medium data were obtained at a constant velocity of U of 1.5 cm./sec. These data were plotted, and, as expected, no effect of frequency on D_L was found.

Others (*13, 14*) state that the experimental and calculated phase angles should check each other. These data were plotted and compared. The maximum deviation between the calculated and experimental phase angles was 16%, and the average was ± 3.4% for all runs with the random porous media. This is a strong indication that the equations and calculation procedures adequately describe the physical situation in the bed. This agreement also indicates that there were no marked end effects in the bed. Only three other investigators (*13, 14, 23*) have reported a close check between experimental and calculated phase angles. Failure to check may be an indication of poor experimental techniques.

The use of frequency response techniques offers one decided advantage of being able to measure the average amplitude of a significant number of inlet and of outlet sine waves under steady state conditions. Another advantage is that the waves are measured at the same time, which helps minimize other variations or errors.

Friction Factor vs. Reynolds Number

In Figure 3 the friction factor f is plotted vs. N'_{Re} for the two random porous media. The line for the 1,000-μ plug shows f proportional to $(N'_{Re})^{-0.45}$. There were not sufficient data to draw accurately the slope of the 2,000-μ line, but it appears to have a slope of about —0.27. However this line was drawn parallel to the 1,000-μ line so that an effective diameter could be determined.

The correlation line from Perry's (*15*) is for uniform granular particles. It is noted that the 1,000- and 2,000-μ data neither fall on one line nor fall on the line from Perry's when the d_p used is the hole grain size for the random porous media. Hence the effective diameter or d_{peff} to use can be estimated by moving both experimental lines on to line C close to the line from Perry's which gives a d_{peff} for the 1,000-μ medium of 640 μ and 587 μ for the 2,000-μ medium. Moving the 2,000-μ line to the 1,000-μ line still gives the same ratio of d_{peff} values. It is interesting to note that the 640- and 587-μ values are close to each other, which may mean that other factors may determine the pressure drop and not the size of the large open holes. The effective diameter concept has often been used to characterize irregular packings or porous structures such as catalysts.

When one plots these data on a plot by Streeter (*24*) for various unconsolidated sands, the data have a N'_{Re} greater than 1.0 and fall near the low range of friction factor values for sands. The slopes are similar to the slopes of the sand data plots. For the sand data and N'_{Re} less than 1.0 the friction factor is proportional to $(N'_{Re})^{-1.0}$ as expected for laminar flow. At a higher Reynold's number the slopes of the lines for sand decrease markedly and are similar to those of the present data. However for the data of Perry (*15*) for beds of granular solids the apparent shift from laminar to turbulent flow occurs at a N'_{Re} of 10 to 20. For the data of Carberry and Bretton (*7*) on beds of spheres the friction factor is also proportional to $(N'_{Re})^{-1.0}$, and at Reynold's numbers above 10 the exponent decreases and becomes less than 1.0.

Effect of Velocity on D_L

A plot was made of the effect of velocity U on D_L. The line for the 1,000-μ medium gives values of D_L about 30% greater than the values for the 2,000-μ line at the same velocities. If D_L is plotted vs. (d_pU), the two lines spread apart very markedly so that the D_L of the 1,000-μ line is about three times that of the 2,000-μ line at the same value of (d_pU).

The above again indicates that the d_p is not the actual grain size of the holes but of some other dimension. It should be realized that this random porous solid is different from even beds of unconsolidated sands, since the present porous solids are literally turned inside out where the grains of sand are the void spaces in the present random porous solid. A plot of D_L vs. N_{Re} would yield the same results as a plot of D_L vs. (d_pU), since the viscosity and density are constant.

In Figure 4 a plot of D_L vs. $(d_{peff}\ U)$ shows that the two lines are only 20% apart compared with a factor of three apart obtained when D_L is plotted vs. (d_pU). The equations for the two lines are as follows for the 1,000- and 2,000-μ beds respectively:

$$D_L = 54.4\ (d_{peff}\ U)^{1.46} \qquad (16)$$

$$D_L = 45.4\ (d_{peff}\ U)^{1.46} \qquad (17)$$

Liles and Geankoplis (*13*) found for all their data

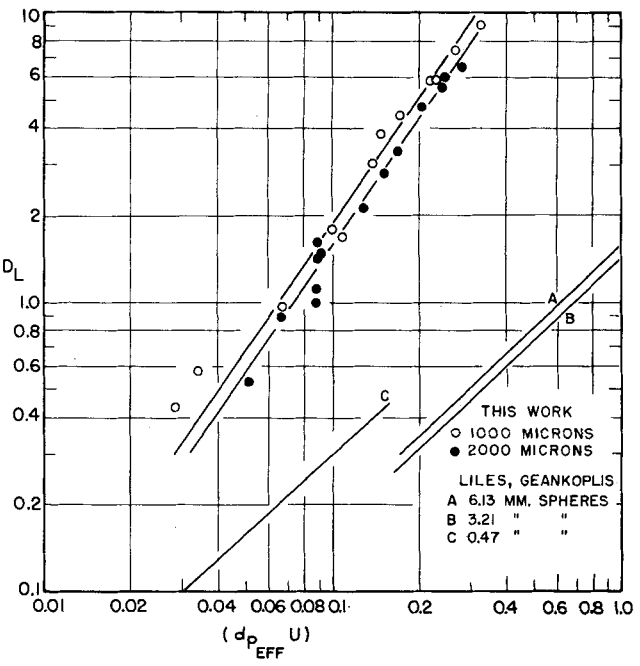

Fig. 4. Effect of $(d_{peff}\ U)$ on D_L.

$$D_L = 1.25\ (d_p)^{0.73}\ U^{0.93} \qquad (18)$$

Carberry and Bretton (7) and Cairns and Prausnitz (5) found D_L proportional to $(N_{Re})^{1.0}$ up to values of N_{Re} of 100 for spheres. Ebach and White (11) found D_L proportional to $(N_{Re})^{1.06}$ up to N_{Re} of 100 for spheres, saddles, and rings. The data of Rafai (16) and Beran (3) for unconsolidated sands show D_L proportional to $U^{1.17}$ to N'_{Re} of about 5.

Hence all other data have a range of exponents on the velocity term of 0.93 to 1.17. This exponent of 1.46 for the present porous media as compared with the range of 0.93 to 1.17 for spheres and other particles may indicate that because of sharp edges of the porous structure there is more mixing in the same length.

It appears that the correlating factor for D_L should not be N_{Re} which includes viscosity but (d_pU). Taylor (25, 26, 27) predicts no effect of viscosity on D_L in laminar flow in capillaries. In turbulent flow in pipes he showed that D_L is proportional to $f^{0.5}$ or, since f is proportional to $(N_{Re})^{-0.2}$, that D_L is proportional to $(\mu)^{0.1}$. This indicates a very weak dependence of D_L on viscosity in pipes.

Ebach and White (11) used propylene glycol-water mixtures and varied the viscosity from 1 to 26 centipoises and found no effect on D_L. However their data were obtained at a N'_{Re} below 0.5 in the laminar region in packed beds of spheres. Experimentally the effect of viscosity on D_L in the turbulent region in packed beds has not been determined, but if an analogy can be drawn to the effect in pipes, then indications are the effect is small in packed beds and porous media.

Pressure Drop and Velocity

In Figure 5 the values of q, which are the same as U', are plotted vs. the pressure drop in centimeters of mercury per centimeters of bed length. The plot indicates that in the lower part of the curve at q less than 0.8 the data do not follow Darcy's law which states q is proportional to $(\Delta P/L)$ [Equation (9)] but give a curved line in the laminar flow region. At higher values of q the data are in the turbulent region. This point corresponds to a N'_{Re} value of 8 to 17 for the two media. For sands (24) this point where turbulence starts is at values of N'_{Re} of 2 to 10 and about 15 for Perry's plot (15) for beds of granular solids.

From Equation (10) the following equations were determined empirically for the 1,000- and 2,000-μ media, respectively, and are plotted as the solid lines in Figure 5:

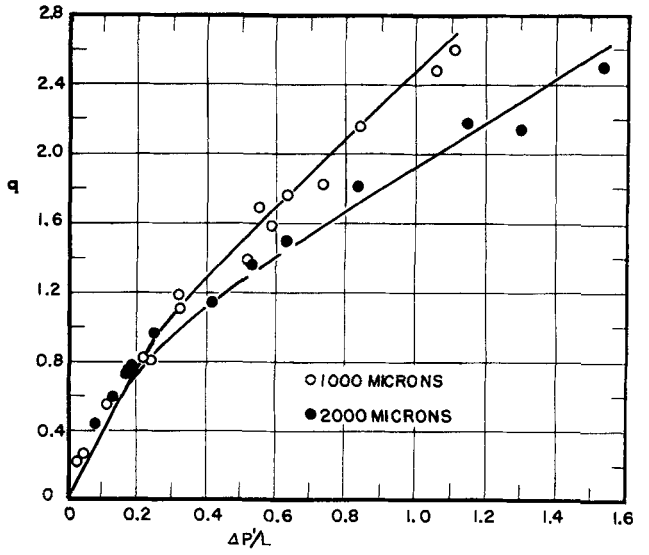

Fig. 5. Pressure drop as a function of velocity.

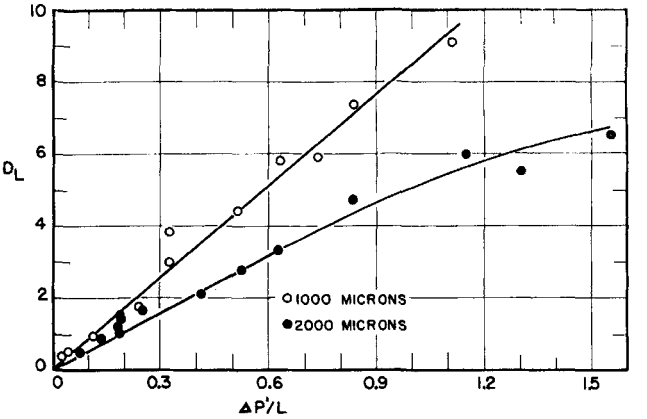

Fig. 6. D_L as a function of pressure drop.

$$\frac{\Delta P'}{L} = 0.247\ q + 0.062\ q^2 \qquad (19)$$

$$\frac{\Delta P'}{L} = 0.247\ q + 0.132\ q^2 \qquad (20)$$

The experimental data follow the equations quite closely except at values of q less than 0.8. At $q = 2.4$ for Equation (19) the kinetic energy losses in the last term are 38.2% of the overall losses.

From Equations (13), (14), (15), and the method of Sherwood and Pigford (21) the values of S', square centimeters surface area per gram of porous material, can be estimated and compared with those calculated by assuming the salt particles are cubes. The data in Table 2 show that the S' values calculated are considerably larger than the values obtained by assuming that the salt crystals are cubes.

Figure 3 shows a greater pressure drop for the present random porous media than equivalent spheres. Hence the S' values as calculated should be larger. This greater pressure drop is probably due to the myriad of sharp corners as seen in the photomicrographs.

D_L and Pressure Drop

In Figure 6 the values of D_L are plotted vs. $(\Delta P'/L)$, and the data show that D_L is proportional approximately to $(\Delta P'/L)^{1.0}$ over the range studied. However for the 2,000-μ line there is some curvature. Since both pressure drop and axial diffusion depend on turbulence, it seems that D_L and pressure drop should be related. It is well known that there is an analogy between mass transfer and momentum transfer. It would be expected that the transition from laminar to turbulent flow would cause curvatures in the line.

Hence it appears that D_L and pressure or momentum drop are related. Much more research is needed to see if this type of relation or analogy holds for all systems and for wide ranges of Reynold's numbers.

Carberry and Bretton (7) also show the same relation in which D_L is proportional to $(\Delta P'/L)^{1.0}$ if one combines their two plots of D_L vs. N_{Re} and f vs. N_{Re} for packed beds.

Comparison of Data on Peclet Numbers

In Figure 7 all the data readily available on beds of spheres, unconsolidated sands, and the present random porous media are plotted as Peclet numbers vs. Reynold's numbers. The present data points are plotted with d_{peff} values.

Beran's data (3) on unconsolidated sands and the present data give similar values of N_{Pe} and are much lower

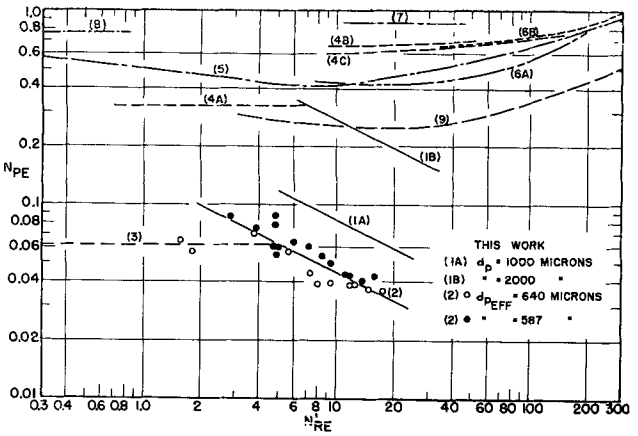

Fig. 7. Peclet number data of various investigators. (1) This work: A. 1,000-μ data; B. 2,000-μ data; (2) This work (using d_{peff}) 0.064 mm. and 0.0587 mm.; (3) Beran (sand); (4) Liles, Geankoplis (spheres) A. 0.47 mm.; B. 3.21 mm.; C. 6.13 mm.; (5) Ebach, White (0.21 to 6.5 mm. spheres); (6) Carberry, Bretton (spheres) A. 3 mm.; B. 5 mm.; (7) Strang, Geankoplis (6 mm. spheres); (8) Rafai (sand); (9) Cairns, Prausnitz (3.2 mm. spheres).

than all other investigators' data. However the Peclèt numbers of the present work decrease with increases in Reynold's number, since D_L is proportional to $U^{1.44}$. In most of the other data the Peclet number remains approximately constant.

The data of Rafai (*16*) for unconsolidated sands are much higher than Beran's data. However Carberry and Bretton (*7*) state that his results may be subject to errors since the experimental results varied depending upon the analytical method used of electrical conductivity or chemical analysis.

If the present data are plotted with the actual d_p as shown by the two solid lines in Figure 7, then the 1,000- and 2,000-μ lines separate and fall much higher and closer to the lines for packed beds.

ACKNOWLEDGMENT

The authors express their appreciation to the General Electric Company, the Dow Chemical Company, and the Koppers Company for financial assistance during the course of this work.

NOTATION

A_o = inlet amplitude concentration, g./ml.
A_1 = outlet amplitude concentration, g./m.
a' = Kozeny constant = 0.50
a = radius of flow channel, cm.
B = ln (A_o/A_1)
C = concentration as a function of position Z and time t, g./ml.
D_L = axial diffusion coefficient, sq.cm./sec.
D = molecular diffusivity, sq.cm./sec.
d_p = diameter of particle, cm.
dc = diameter of flow channel, cm.
d_{peff} = effective diameter of particle, cm.
f = friction factor, dimensionless.
K = constant in Equation (7)
K_2 = constant in Equation (10)
k = specific permeability, sq.cm.
l = length of dead-end pore, cm.
L = length of porous medium, cm.
N_{Pe} = Peclet number, d_pU/D_L
N_{Re} = Reynolds number, $d_pU\rho/\mu$
N_{ReC} = Reynolds number, $(dcUc\ \rho/\mu)$
N'_{Re} = Reynolds number, $d_pU'\ \rho/\mu$
N_{Reeff} = Reynolds number, $(d_{peff}\ U\ \rho/\mu)$
ΔP = pressure drop, g./sq.cm.
$\Delta P'$ = pressure drop, cm. Hg.
q = open tube velocity, cm./sec.
S = sq. cm. surface/cc. volume porous material
S_o = sq. cm. surface/cc. solid material
S' = sq. cm. surface/g. porous material
t = time, sec.
T = tortuosity factor = 1.5.
U = interstitial velocity, cm./sec.
Uc = actual flow channel velocity, cm./sec.
U' = open tube velocity, cm./sec.
Z = bed distance from inlet, cm.

Greek Letters

β = constant in Equation (7)
ϵ = porosity or void fraction
ξ_{calc} = calculated phase angle shift, rad.
ξ_{exp} = experimental phase angle shift, rad.
μ = viscosity, poises
ρ = density, g./ml.
ω = frequency of sine wave, rad./sec.

LITERATURE CITED

1. Aris, R., *Chem. Eng. Sci.*, **10**, 80 (1959).
2. *Ibid.*, **11**, 194 (1959).
3. Beran, M. J., Ph.D. dissertation, Harvard Univ., Cambridge, Massachusetts (1955).
4. Blackwell, R. J., J. R. Rayne, and W. M. Terry, *Trans. Am. Inst. Mining, Met., Petrol. Engrs.*, **216**, 1 (1959).
5. Cairns, E. J., and J. M. Prausnitz, *Chem. Eng. Sci.*, **12**, 20 (1960).
6. ————, *Ind. Eng. Chem.*, **51**, 1441 (1959).
7. Carberry, J. J., and R. H. Bretton, *A.I.Ch.E. Journal*, **4**, 367 (1958).
8. Carslow, H. S., and J. C. Jaeger, "Conduction of Heat in Solids," 2 ed., Oxford Press, London, England (1959).
9. Converse, A. C., *A.I.Ch.E. Journal*, **6**, 344 (1960).
10. Deisler, P. F., Jr., and R. H. Wilhelm, *Ind. Eng. Chem.*, **45**, 1219 (1953).
11. Ebach, E. A., and R. R. White, *A.I.Ch.E. Journal*, **4**, 161 (1958).
12. Ergun, Sabri, *Chem. Eng. Progr.*, **48**, 88 (1952).
13. Liles, A. W., and C. J. Geankoplis, *A.I.Ch.E. Journal*, **6**, 591 (1960).
14. McHenry, K. W., Jr., and R. H. Wilhelm, *ibid.*, **3**, 83 (1957).
15. Perry, J. H., "Chemical Engineers' Handbook," McGraw-Hill, New York (1950).
16. Rafai, M. N. E., Ph.D. dissertation, Univ. Calif., Berkeley, California (1956).
17. Rosen, J. B., and W. E. Winsche, *Chem. Phys.*, **18**, 1587 (1950).
18. Saffman, P. G., *Chem. Eng. Sci.*, **11**, 125 (1959).
19. ———, *J. Fluid Mech.*, **6**, 321 (1959).
20. Scheidegger, A. E., "The Physics of Flow Through Porous Media," MacMillan, New York (1960).
21. Sherwood, T. K., and R. L. Pigford, "Absorption and Extraction," McGraw-Hill, New York (1952).
22. Stahel, E. P., Ph.D. dissertation, Ohio State Univ., Columbus, Ohio (1962).
23. Strang, D. A., and C. J. Geankoplis, *Ind. Eng. Chem.*, **50**, 1305 (1958).
24. Streeter, V. L., "Handbook of Fluid Dynamics," McGraw-Hill, New York (1961).
25. Taylor, G. I., *Proc. Roy. Soc. (London)*, **225A**, 473 (1954).
26. *Ibid.*, **219A**, 186 (1954).
27. *Ibid.*, **223A**, 446 (1954).
28. Tek, M. R., *J.P. Tech.*, **9**, 45 (June, 1957).
29. Turner, G. A., *Chem. Eng. Sci.*, **7**, 156 (1958).
30. *Ibid.*, **10**, 14 (1959).
31. Von Rosenberg, D. V., *A.I.Ch.E. Journal*, **2**, 55 (1956).

Manuscript received August 7, 1962; revision received July 26, 1963; paper accepted July 31, 1963.